Fuzzy interacting multiple model H∞ particle filter algorithm based on current statistical model

Wang, Q., Chen, X., Zhang, L., Li, J., Zhao, C. and Qi, M.

Fuzzy Interacting Multiple Model H∞ Particle Filter Algorithm Based on Current Statistical Model

Qicong Wang[1,2] · Xiaoqiang Chen[1] · Lin Zhang[3] · Jin Li[1] · Chong Zhao[1] ·
Man Qi[4]

Abstract In this paper, fuzzy theory and interacting multiple model are introduced into H∞ filter-based particle filter to propose a new fuzzy interacting multiple model H∞ particle filter based on current statistical model. Each model uses H∞ particle filter algorithm for filtering, in which the current statistical model can describe the maneuver of target accurately and H∞ filter can deal with the nonlinear system effectively. Aiming at the problem of large amount of probability calculation in interacting multiple model by using combination calculation method, our approach calculates each model matching probability through the fuzzy theory, which can not only reduce the calculation amount, but also improve the state estimation accuracy to some extent. The simulation results show that the proposed algorithm can be more accurate and robust to track maneuvering target.

Keywords Fuzzy theory · Interacting multiple model · Particle filter · H∞ filter

✉ Qicong Wang
qcwang@xmu.edu.cn

1 Department of Computer Science, Xiamen University, Xiamen 361005, China

2 Shenzhen Research Institute, Xiamen University, Shenzhen 518000, China

3 Xiamen City Management Administrative Enforcement Bureau, Xiamen 361000, China

4 Department of Computing, Canterbury Christ Church University, Kent CT1 1QU, UK

1 Introduction

When the target is maneuvering, filtering residual (innovation) will change. The size of filtering residual is closely related to the maneuvering magnitude of the target. In the interacting multiple model (IMM) algorithm, filtering residuals exist not only in the estimation of each model, but also in the matching probability of the model. The matching probability of the models determines the weights of the filter estimates of each model in the fusion output, which has a great impact on the tracking accuracy of the target. In the algorithm, the state of the model is uncertain, and its matching probability is obtained by combination calculation. The method has exponential complexity and a large amount of calculation. In addition, the current statistical model can improve the acceleration with zero mean of Singer model for the adaptive acceleration mean. However, the scope change of target acceleration is limited in the current statistical model, when the target motion state changes or mutations, the tracking accuracy will be reduced significantly. This can result in the following dilemma. On the one hand, in order to improve performance, we need to add the number of models. On the other hand, increasing the number of models may not only not improve the system performance, but also greatly increase the amount of computation. At this time, if the model probability of IMM algorithm is taken as the input of the fuzzy inference system, we can choose a subset of more realistic model from the model set through the fuzzy logic reasoning. Thus, some unnecessary models can be eliminated to reduce the competition among models. In the proposed approach, the model matching probability is obtained by using the fuzzy theory instead of the original combination calculation method. The uncertainty of measurement space is taken into account, and the reasoning

from the uncertainty of measurement space to the uncertainty of mode space can be solved. The application of fuzzy theory not only can reduce the computational complexity of the algorithm to some extent, but also improve the accuracy of motion state estimation for maneuvering target.

2 Related Work

For dynamic state estimation, the interacting multiple model (IMM) algorithm is a very effective method [1–4]. Through the Markov transition probability, this method is characterized by switching multiple models, adjusting the filter bandwidth automatically and tracking arbitrary maneuvering of the target. In the traditional methods, each model filter usually uses Kalman filter or extended Kalman filter algorithm. For nonlinear and non-Gaussian system, their filtering performance can be degenerated greatly. In recent years, the particle filter has been widely applied to target tracking, which can solve the nonlinear and non-Gaussian problems [5, 6], so the interacting multiple model particle filter (IMMPF) algorithms are proposed for the strong maneuvering target tracking [7, 8]. However, the standard particle filter algorithm uses the system state transition probability as its importance density function, which cannot utilize the latest observations to generate new particles. The result is that the produced particle samples focus on the last of the posterior probability distribution, which leads to a blind choice in the particles and causes the reduction in the filtering precision [9]. In addition, the particle filter usually adopts a large number of particles which will produce a lot of calculation amount and influence real-time tracking. Some methods can optimize performance using distributed technologies such as Top-k or EMP [10–14]. In this paper, we introduce H∞ filter [15–17], which has strong robustness in external interference and reduces the linearization error of nonlinear filtering, into the framework of particle filter. At the same time, by incorporating the latest observation information into importance density function, it can better approach the posterior probability distribution of the real state.

At present, dynamic modes of many control systems are becoming more and more complex. The choice of the motion model is one of the important factors affecting the tracking accuracy. The closer the model is to the actual motion mode of the target, the better the tracking performance will be. It is very difficult to describe the system dynamics accurately with mathematical models. Therefore, more and more researchers try to use the theory of fuzzy control to solve the problem that complex systems are difficult to model accurately [18–20]. For example, to improve object tracking from video sequences, a fuzzy observation model-based particle filter is proposed to exploit spatial correlation in a rough set-theoretic framework [19]. To deal with misleading state estimation, fuzzy system is introduced into IMM filter to solve the fault-prognostic problem [20]. In this paper, we use the theory of fuzzy control to calculate the matching probability of the model. The membership function is centered on the filter value of each model at that time, and the observation value at that time is transformed into independent variable. Two function values are obtained and normalized as the probability of the model. This method not only reduces the computational complexity of the algorithm, but also improves the tracking accuracy.

3 The Current Statistical Model

Assuming that a is random acceleration of target, $a_{max} \geq 0$, $a_{-max} < 0$ are, respectively, upper limit and lower limit of the acceleration. We can use the following situations to modify probability density function.

(1) When $a_{-max} < a < 0$, the probability density, the mean and variance of the acceleration as follows:

$$P_r(a) = \frac{a - a_{-max}}{\mu^2} \exp\left[-\frac{(a - a_{-max})^2}{2u^2}\right] \quad (1)$$

$$E(a) = a_{-max} + \sqrt{\frac{\pi}{2}}\mu \quad (2)$$

$$\sigma_a^2 = \frac{4 - \pi}{2}\mu^2 \quad (3)$$

(2) When $0 < a < a_{max}$, the probability density, the mean and variance of the acceleration as follows:

$$P_r(a) = \frac{a_{max-} - a}{\mu^2} \exp\left[-\frac{(a_{max} - a)^2}{2u^2}\right] \quad (4)$$

$$E(a) = a_{max} - \sqrt{\frac{\pi}{2}}\mu \quad (5)$$

$$\sigma_a^2 = \frac{4 - \pi}{2}\mu^2 \quad (6)$$

(3) When $a = 0$, the probability density function can be expressed as follows:

$$P_r(a) = \delta(a) \quad (7)$$

(4) When $a = a_{max}$ or $a = a_{-max}$, the probability density function is 0. The current statistical model of maneuvering t current statistical model of maneuvering target is described as follows:

$$\begin{bmatrix} x(\dot{t}) \\ x(\ddot{t}) \\ x(\dddot{t}) \end{bmatrix} = \begin{bmatrix} 0 & 1 & 1 \\ 0 & 0 & 0 \\ 0 & 0 & -a \end{bmatrix} \begin{bmatrix} x(t) \\ x(\dot{t}) \\ x(\ddot{t}) \end{bmatrix} + \begin{bmatrix} 0 \\ 0 \\ a \end{bmatrix} \overline{a}(t) + \begin{bmatrix} 0 \\ 0 \\ 1 \end{bmatrix} w(t) \tag{8}$$

where the x, $x(\dot{t})$ and $x(\ddot{t})$, respectively, represent the location, velocity and acceleration of the target motion, and $x(\dddot{t})$ is the derivative of acceleration. $\overline{a}$ is the acceleration mean, a is maneuvering frequency, the mean value of $w(t)$ is zero and variance of white noise is $\sigma_w^2 = 2a\sigma_a^2$.

If set sampling interval as T, discrete variance can be expressed as follows:

$$X(k + 1) = F(k)X(k) + G(k)\overline{a} + v(k) \tag{9}$$

where $F(k)$'s value and $F(k)$'s value of the Singer model are equal, and $G(k)$'s value is expressed as follows:

$$G(k) = \begin{bmatrix} \frac{1}{a}(-T + \frac{aT^2}{2} + \frac{1 - e^{-aT}}{a}) \\ T - \frac{1 - e^{-aT}}{a} \\ 1 - e^{-aT} \end{bmatrix} \tag{10}$$

The covariance of discrete-time process noise $w(t)$ is as follows:

$$Q(k) = 2a\sigma_a^2 \begin{pmatrix} q_{11} & q_{12} & q_{13} \\ q_{21} & q_{22} & q_{23} \\ q_{31} & q_{32} & q_{33} \end{pmatrix} \tag{11}$$

where

$$q_{11} = \frac{1}{2a^5}[1 + 2aT - e^{-2aT} + 2a^3T^3/3 - 2a^2T^2 - 4aTe^{-aT}]$$
$$q_{12} = \frac{1}{2a^4}[1 - 2e^{-aT} + e^{-2aT} + 2aTe^{-aT} - 2aT + 2a^2T^2] = q_{21}$$
$$q_{13} = \frac{1}{2a^3}[1 - e^{-2aT} - 2aTe^{-aT}] = q_{31}$$
$$q_{22} = \frac{1}{2a^3}[-3 + 4e^{-aT} - e^{-2aT} + 2aT]$$
$$q_{23} = \frac{1}{2a^2}[1 - 2Te^{-aT} + e^{-2aT}] = q_{32}$$
$$q_{33} = \frac{1}{2a}[1 - 2e^{-2aT}]$$
$$\tag{12}$$

When the absolute values of $a_{\max}$ and $a_{-\max}$ are small, the variance of system state noise is also small, and tracking precision is high. However, the scope change of the maneuvering target is relatively small, the corresponding response speed is also slow. When the absolute values of $a_{\max}$ and $a_{-\max}$ are large, the variance of system state noise is large as well. If the scope change of the maneuvering target becomes larger, the response speed will also become faster, that is, tracking algorithm for larger scope

maneuvering can respond quickly. The current statistical model is a good practical model which can reflect the scope and intensity changes of the maneuvering target.

4 H∞ Particle Filter Algorithm

In the particle filter, we can choose some different proposal distribution functions. The most commonly used function is the prior density [21, 22], that is, $q(x_k^i|x_{k-1}^i, z_k) = p(x_k^i|x_{k-1}^i)$. However, its shortcomings are also obvious that it does not consider the system current measurements, which can lead to the particle degeneracy problem. To this end, the proposed approach utilizes H∞ algorithm to generate new particles, which can consider the system current measures to solve impoverishment problem and improve the filtering accuracy. The algorithm is described as follows.

Step 1: Initialization Sample the initial particles $x_0^{(1)}, x_0^{(2)}, \ldots, x_0^{(N)}$, where N is the number of particles, and $\omega_0^i = 1/N, i = 1, 2, \ldots N$.

Step 2: H ∞ filter We bring the particles at time $k - 1$ into the H∞ filter, and then each particle performs H∞ filtering to obtain the predicted particle at time k. H∞ filter is described as follows.

$$x(k|k - 1) = \Phi(k|k - 1)x(k - 1) \tag{13}$$

$$p(k|k - 1) = \Phi(k|k - 1)p(k - 1)\Phi^T(k - 1) + \Gamma(k - 1)\Gamma^T(k - 1) \tag{14}$$

$$x(k) = x(k|k - 1) + K_\infty(k - 1)\begin{bmatrix} Z(k) - H(k)x(k|k - 1) \\ \tilde{S}(k) - L(k)x(k|k - 1) \end{bmatrix} \tag{15}$$

$$K_\infty(k) = p(k|k - 1)\begin{bmatrix} H^T(k) & L^T(k) \end{bmatrix} R_e^{-1}(k) \tag{16}$$

$$p(k) = (I - K_\infty(k)[H(k) \quad L(k)])p(k|k - 1) \tag{17}$$

$$R_e(k) = \begin{bmatrix} I & 0 \\ 0 & -\gamma^2 I \end{bmatrix} + \begin{bmatrix} H(k) \\ L(k) \end{bmatrix} p(k|k - 1)\begin{bmatrix} H^T(k) & L^T(k) \end{bmatrix} \tag{18}$$

The above formulas constitute the H∞ robust filter algorithm. Because of using the different filter gain, the H∞ filter is different from the standard Kalman filter essentially. When the disturbance attenuation factor $\gamma \to \infty$, we can see that $M(k) \to 0$, which makes the H∞ filter recursion degenerate into the Kalman filter recursion. So the H∞ norm of the Kalman filter may be very large, which result in poor robustness performance. As the disturbance attenuation factor $\gamma \to \min$, we find $M(k) \to I$, where I is the identity matrix. Though we can get good robustness, the estimation square error is quite large. We can obtain

satisfactory requirement by adjusting the parameter γ according to testing experiment in practice.

When we obtain the target observation at time k, we can calculate the importance weight of each predicted particle, and then their weights are normalized.

$$\omega_k^i = \omega_{k-1}^i \frac{p(z_k|x_k^i)p(x_k^i|x_{k-1}^i)}{q(x_k^i|x_{k-1}^i, z_k)} \tag{19}$$

$$\tilde{\omega}_k^i = \omega_k^i / \sum_{j=1}^N \omega_k^i \tag{20}$$

where $q(x_k^i|x_{k-1}^i, z_k)$ is the importance density function, generally, $q(x_k^i|x_{k-1}^i, z_k) = p(x_k^i|x_{k-1}^i)$. After normalizing the weight, we can get the approximate posterior distribution $p(x_k|z_{1:k})$. $\delta(.)$ is the Dirac function.

$$p(x_k|z_{1:k}) = \sum_{j=1}^N \tilde{\omega}_k^i \delta(x_k - x_k^i) \tag{21}$$

Step 3: Resampling Accept the particles that have high importance weights, and eliminate the particles that have low importance weights. Set the weights $\omega_k^i = 1/N$, $i = 1,\ldots,N$.

Step 4: Output calculation The posterior probability estimation of the state is obtained as

$$\hat{x}_k \approx \sum_{i=1}^N \tilde{\omega}_k^i x_k^i \tag{22}$$

Step 5 $k = k + 1$, and move to step2.

5 Fuzzy Interactive Multiple Model H∞ Particle Filter Algorithm Based on Current Statistical Model

For the interactive multiple model, the proposed approach calculates each model matching probability by using the fuzzy control theory, finally fusion output. The concrete realization of the fuzzy control theory in algorithm is as follows. First, the filtering values of models at current time are regarded as the center of the membership functions, respectively, and establish membership functions. Second, the observation at this time is converted into the independent variable. Finally, we can obtain function values as the model probability after normalizing. The flowchart of the proposed algorithm is showed in Fig. 1.

From Fig. 1, it is seen that this algorithm can be divided into three parts, namely IMM filtering, calculating model matching probability by the fuzzy inference system and fusion output. The three parts are described as follows.

Step1: IMM filtering In this step, the particles are initialized. Sample the initial particles $x_0^{(1)}, x_0^{(2)}, \ldots, x_0^{(N)}$,
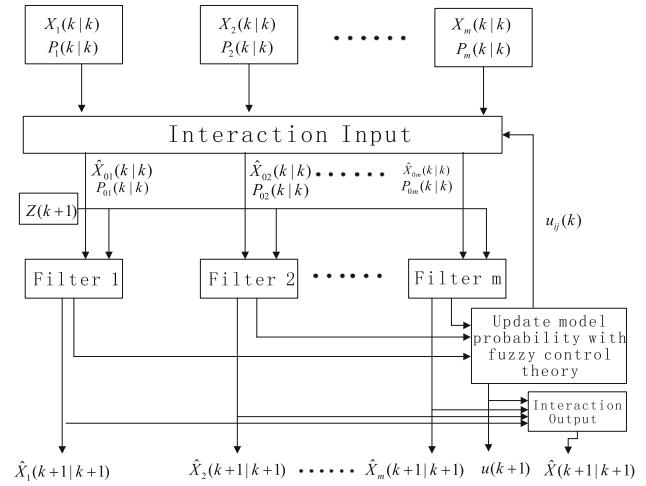

Fig. 1 The flowchart of the proposed algorithm

where N is the number of particles, and M is the number of models. Set the initial value $U = u_m^i(0)_{m=1,2,\cdots,M}^{i=1,2\cdots N}$, where $u_m(k)$ represents the model probability, $\sum u_m = 1$. For input interaction, the particles of each model perform interacting operation:

$$u_{n/m}(k) = \frac{1}{c}\pi_{nm}u_n(k) \tag{23}$$

$$\bar{c}_m = \sum \pi_{nm}u_n(k) \tag{24}$$

$$\hat{x}_{0m}^N(k/k) = \sum_{n-1}^N \hat{x}_n^N(k/k)u_{n/m}^N(k) \tag{25}$$

$$p_{0m}^N(k/k) = \sum_{n-1}^N u_{n/m}^N(k)\{p_n^N(k/k) + [\hat{x}_n^N(k/k)] \\ - \hat{x}_{0m}^N(k/k)][\hat{x}_n^N(k/k)] - \hat{x}_{0m}^N(k/k]^T\} \tag{26}$$

where $\hat{x}_{0m}^N(k/k)$ and $p_{0m}^N(k/k)$, respectively, represent the covariance matrix and the mixed state vector of the $N - th$ particle of model m at time k. After interacting computing, the state vector $\hat{x}_m(k+1/k+1)$, weight $w_m^N(k+1)$ and the covariance matrix $p_m(k+1/k+1)$ of model m at time k+1 are estimated by H∞ particle filter.

Step2: Calculating model matching probability by the fuzzy inference system The measurement value z at the current time is the direct input. According to z, we can obtain W_m which is the direct input of the fuzzy inference system, and the calculation of W_m is as follows:

$$DD_m(k) = [abs(z(1,k) - x_m(1,k)) - abs(z(3,k) - x_m(3,k))] \\ * [abs(z(1,k) - x_m(1,k)) - abs(z(3,k) - x_m(3,k))]^T \tag{27}$$

$$W_m = DD_m / \Sigma_{m-1}^M DD_m \tag{28}$$

This paper only adopts two motion models, therefore $m = 2$. The two fuzzy systems are carried out simultaneously, in which the input z is converted to $DD_m(k)$, and

$DD_m(k)$ is converted into fuzzy input value W_m of fuzzy systems by fuzzy equation $DD_m/\Sigma_{m-1}^{M}DD_m$. Finally, unify two fuzzy outputs.

Assume that the universal space of W_m is A_m, and two different models in model set have the same universal space. The fuzzy subset size of the fuzzy inference system is a great impact on calculation amount. Generally, the more fuzzy subsets, the larger computation amount, but the higher precision. We define fuzzy subset of the input W_m on the universal as SP (small positive), MP (middle positive) and LP (large positive). The commonly used Gaussian function $u(W_m) = \exp[\frac{-(W_M-C)^2}{2\sigma^2}]$ is applied as membership function. As shown in Fig. 2, c and σ are distribution parameters of quantitative input of the fuzzy inference system. After fuzzy inference, we can obtain fuzzy value w_m of W_m. Fuzzy subset of the fuzzy output space is defined as SP (small positive), MP (middle positive), and LP (large positive), and common trigonometric function is treated as membership function.

In the left-hand subgraph of Fig. 2, the abscissa represents value of W_m, and the ordinate represents the degree of membership. In the other subgraph, the abscissa is the value of the output probability, and the ordinate is the degree of membership. The essence of the fuzzy control theory is when fuzzy input values correspond to the two membership values at the same time; the corresponding two results are combined into the final output. After fuzzification, the model matching probability can be adjusted by the following fuzzy rules in Table 1.

According to the above fuzzy rules, we can obtain the model matching probability at the current time. After the model is normalized, the final fuzzy matching probability of model is calculated by

$$u_i = \frac{u_i}{\sum_{i=1}^{m} u_i} \qquad (29)$$

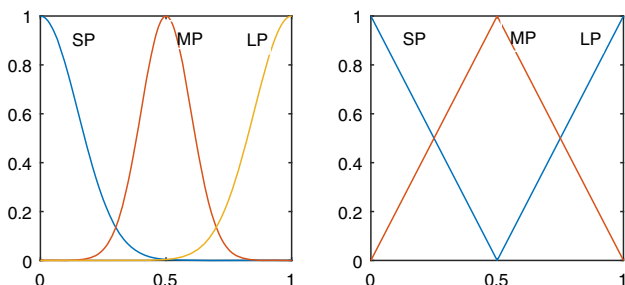*Step 3: Fusion output* State at time k+1 is estimated by

Table 1 Fuzzy relationship table

Rule	W_1	W_1	u_1	u_2
R_1	SP	MP	LP	SP
R_2	SP	LP	LP	SP
R_3	MP	SP	SP	LP
R_4	MP	LP	SP	SP
R_5	LP	SP	SP	LP
R_6	LP	MP	SP	SP

$$\hat{x}_m(k+1|k+1) = \sum_{i=1}^{N} u_i(k+1)\hat{x}_m^i(k+1|k+1) \qquad (30)$$

State covariance matrix at time k+1 is computed by

$$P_m(k+1|k+1) = \sum_{i=1}^{N} u_i(k+1)$$
$$\left\{ P_m^i(k) + [\hat{x}_m^i(k+1|k+1) - \hat{x}_m(k+1|k+1)][.]^T \right\} \qquad (31)$$

6 Simulation Results and Analysis

In order to validate the performance of interacting multiple model H∞ particle filtering (FIMMCVCS-H∞PF) based on current statistical model, we compare it with two algorithms. They are, respectively, the fuzzy interacting multiple model particle filtering based on current statistical model (FIMMCVCS-PF) and the fuzzy interacting multiple model Kalman particle filtering algorithm-based current statistical model (FIMMCVCS-KPF). Simulation experiments are carried on two different motion trajectories. In case 1, target performs weak maneuvering motion whose nonlinear level is not very high. In case 2, target performs strong maneuvering motion whose nonlinear level is high. In the IMM algorithm, there should be at least one target maneuver model and one non-maneuver model. The system model and observation model of two scenes are the same, so we use the uniform model (CV) and the current statistical model (CS) for the IMM filtering. Why we use these models is that uniform model perform well on non-maneuver model and the current statistical model do well on target maneuver model. The system model and observation models are described as follows.

System model

$$x(k+1) = f(x(k), T, M_k) + w(x(k), M_k) \qquad (32)$$

Observation model

$$z(k+1) = h(x(k+1), T) + v(x(k+1)) \qquad (33)$$

where $x = [x, x, y, y, a, a]^T$ is the state vector, $s = [x, y]^T$ is the position vector, $v = [x, y]^T$ is the velocity vector, $a =$

Fig. 2 Membership function of the input space and the output space

$[a, a]^T$ is the acceleration vector, and the system noise is Gaussian white noise w with zero mean.

Here, we use the uniform model (CV) as a model M_1, and the current statistical model (CS) as the other model M_2. The two models are described as follows

$$f(x(k), T, M_1) = \begin{bmatrix} 1 & T & 0 & 0 & 0 & 0 \\ 0 & 1 & 0 & 0 & 0 & 0 \\ 0 & 0 & 1 & T & 0 & 0 \\ 0 & 0 & 0 & 1 & 0 & 0 \\ 0 & 0 & 0 & 0 & 0 & 0 \\ 0 & 0 & 0 & 0 & 0 & 0 \end{bmatrix} x(k) + w_1(k)$$

(34)

$$f(x(k), T, M_2) = \begin{bmatrix} 1 & T & 0 & 0 & T^2/2 & 0 \\ 0 & 1 & 0 & 0 & T & T^2/2 \\ 0 & 0 & 1 & T & 0 & 0 \\ 0 & 0 & 0 & 1 & 0 & T \\ 0 & 0 & 0 & 0 & 1 & 0 \\ 0 & 0 & 0 & 0 & 0 & 1 \end{bmatrix} x(k) + w_2(k)$$

(35)

Observation model is polar coordinate model. Its expression is

$$Z(k) = \begin{bmatrix} r(k) \\ \varphi(k) \end{bmatrix} = h(x(k)) + v(k) = \begin{bmatrix} \sqrt{x(k)^2 + y(k)^2} \\ arctan(\frac{x(k)}{y(k)}) \end{bmatrix} + \begin{bmatrix} v_r(k) \\ v_\varphi(k) \end{bmatrix}$$

(36)

Assume that the position of the radar in origin, $v(k)$ is Gaussian white noise with zero mean, whose covariance matrix is $R(k) = diay(\sigma_r^2, \sigma_\varphi^2)$, where σ_r is standard deviation of the distance, and σ_φ is standard deviation of the angle.

In two cases, the initial position of the target is $x(0) = [100\,\text{m}, 120\,\text{m}]^T$, initial velocity is $v(0) = [15\,\text{m/s}, 15\,\text{m/s}]^T$, the initial acceleration is $a(0) = [0\,\text{m}^2/\text{s}, 0\,\text{m}^2/\text{s}]^T$ scan cycle is $T = 1$ s, the particle number is $N = 100$, model probability is $u_1(0) = 0.5$, $u_2(0) = 0.5$ at initial time and probability transition matrix is $\Pi = \begin{bmatrix} 0.8 & 0.2 \\ 0.2 & 0.8 \end{bmatrix}$.

6.1 Simulation Experiment 1

In this section, we show comparisons between algorithms using fuzzy control and those without fuzzy control theory, which mainly demonstrates the efficiency of the fuzzy theory in the maneuvering target tracking. Maneuvering target performs a total of 100 scan cycles, in which 1–28 scan cycles are uniform motion, 29–70 scan cycles are turn motion and the remaining 30 scan cycles are uniform motion. The turn rate is $w = 0.13$ rad/s, disturbance attenuation factor of H∞ particle filter is $\gamma = 0.7$. Because our model is 2D, here we use the distance error, which is the difference between the estimated state and the real state. If this method is used in more difficult issue, the error assessment can be adjusted. The simulation results as follows.

From Figs. 3, 4 and 5, we can see that the interacting multiple model particle filter algorithm can improve the accuracy of target tracking because of using the fuzzy control theory. In particular, when the target performs maneuvering motion, the tracking performance of the algorithm with fuzzy control theory is greatly enhanced. From Figs. 6, 7, 8, 9, 10 and 11, it is seen that the interacting multiple model Kalman particle filter and the interacting multiple model H∞ particle filter can improve the tracking performance to some extent by the fuzzy control theory. Because IMMCVCS-KPF and IMMCVCS-H∞PF algorithm originally have good performance for maneuvering target tracking, the advantages of the fuzzy control theory are not obvious for the two algorithms. But the application of fuzzy control theory can reduce the computational complexity.

6.2 Simulation Experiment 2

In this section, we show the performance comparisons among three algorithms, namely FIMMCVCS-PF, FIMMCVCS-KPF and FIMMCVCS-H∞PF. The main purpose of experiments is to demonstrate the effectiveness of the proposed FIMMCVCS-H∞PF in this paper.
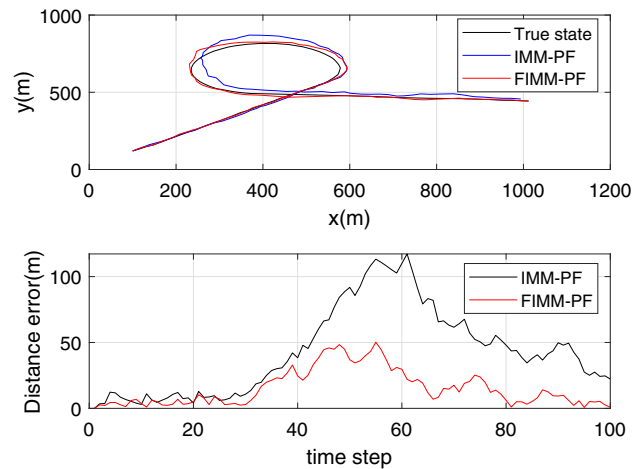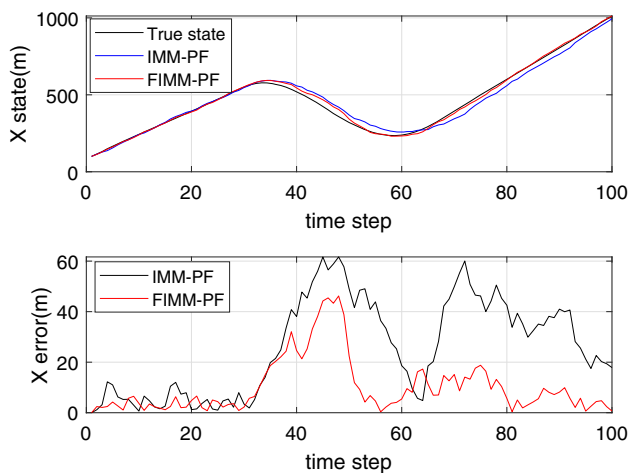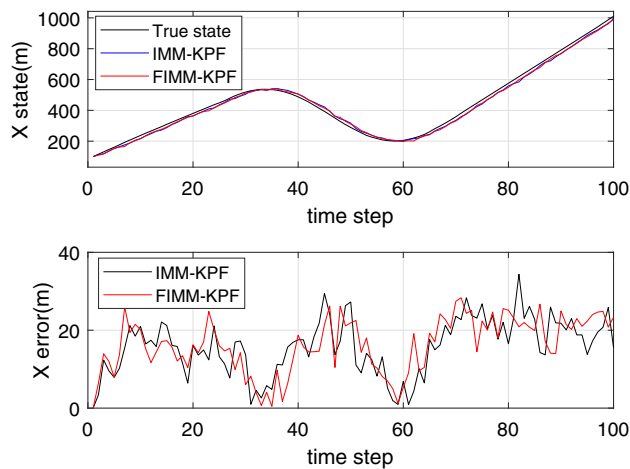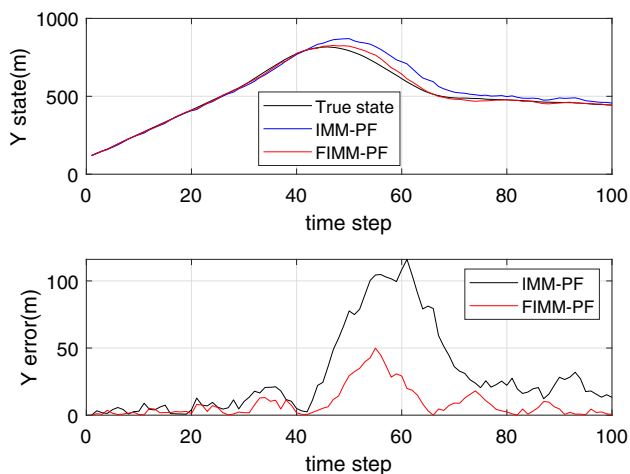

Fig. 3 Trajectory and position error comparison between IMMCVCS-PF and FIMMCVCS-PF filter
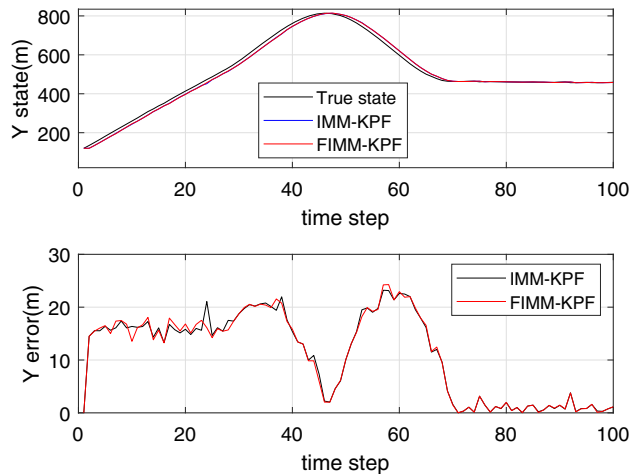
Fig. 4 Trajectory and position error comparison between IMMCVCS-PF and FIMMCVCS-PF filter in the X-direction
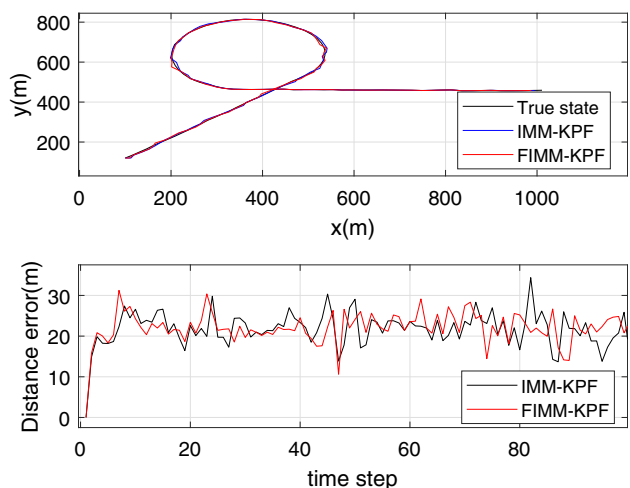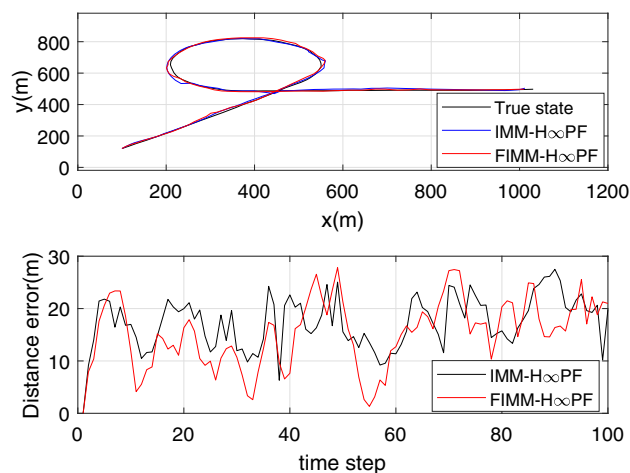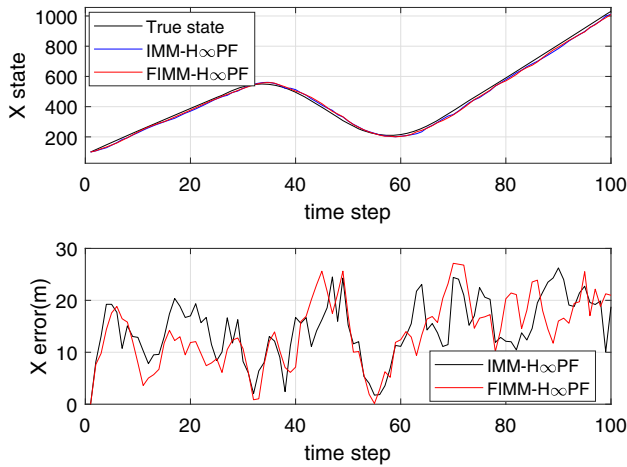

Fig. 5 Trajectory and position error comparison between IMMCVCS-PF and FIMMCVCS-PF filter in the Y-direction

Fig. 6 Trajectory and position error comparison between IMMCVCS-KPF and FIMMCVCS-KPF filter

Fig. 7 Trajectory and position error comparison between IMMCVCS-KPF and FIMMCVCS-KPF filter in the X-direction

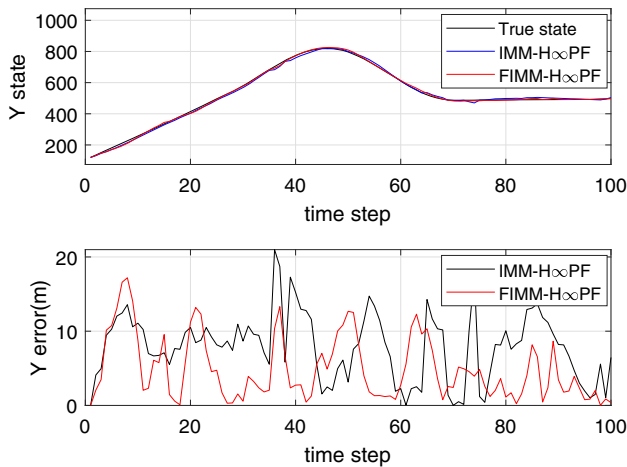**Fig. 8** Trajectory and position error comparison between IMMCVCS-KPF and FIMMCVCS-KPF filter in the Y-direction

Fig. 9 Trajectory and position error comparison between IMMCVCS-$H\infty$PF and FIMMCVCS-$H\infty$PF filter

Fig. 10 Trajectory and position error comparison between IMMCVCS-$H\infty$PF and FIMMCVCS-$H\infty$PF filter in the X-direction


Fig. 11 Trajectory and position error comparison between IMMCVCS-$H\infty$PF and FIMMCVCS-$H\infty$PF filter in the Y-direction

6.2.1 Weak Maneuvering Target Tracking Situation

Maneuvering target performs a total of 100 scan cycle, where 1–28 scan cycles are uniform motion, 29–70 cycles are turn motion, and the remaining 30 scan cycles are uniform motion. The turn rate is $w = 0.08$ rad/s, and disturbance attenuation factor of $H\infty$ particle filter is $\gamma = 0.7$.

From Figs. 12, 13, 14 and 15, we can see that the FIMMCVCS-$H\infty$PF is obviously better than FIMMCVCS-PF and FIMMKPF. FIMMCVCS-KPF and FIMMCVCS-$H\infty$PF can handle target maneuvering motion effectively. The tracking errors of three algorithms are all reduced. When the target does non-maneuvering motion, FIMMCVCS-PF can track the target well and tracking accuracy is similar with FIMMCVCS-KPF and FIMMCVCS-$H\infty$PF. However, when the target maneuvering happens, although the maneuvering of this scene is weak, the tracking error of FIMMCVCS-PF is still far lager
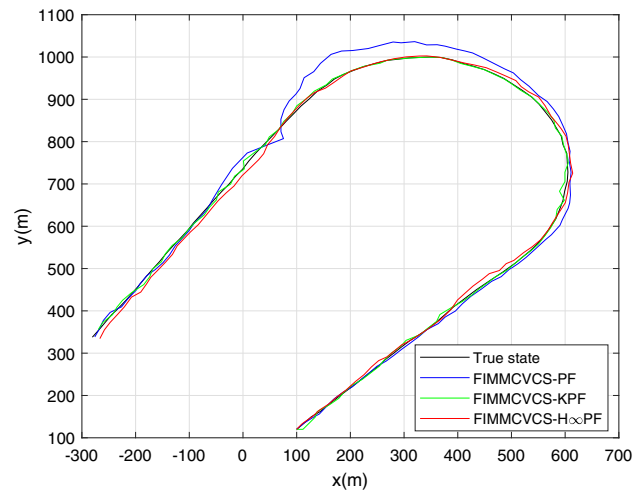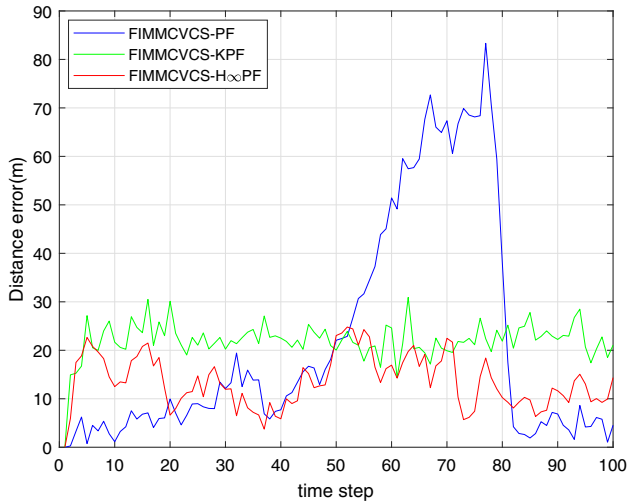

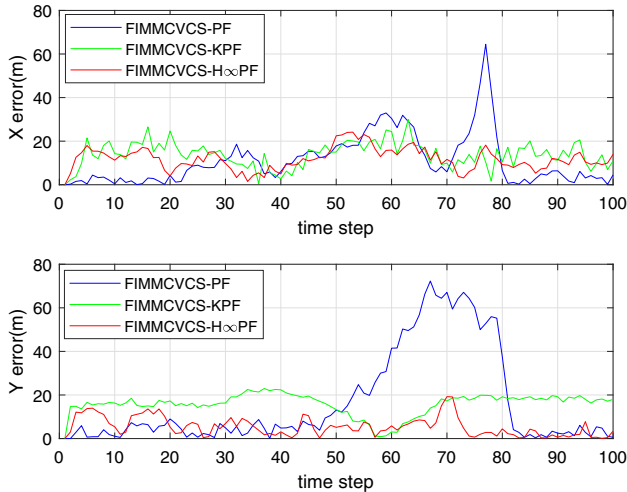**Fig. 12** Trajectory comparison of FIMMCVCS-PF, FIMMCVCS-KPF and FIMMCVCS-$H\infty$PF filter
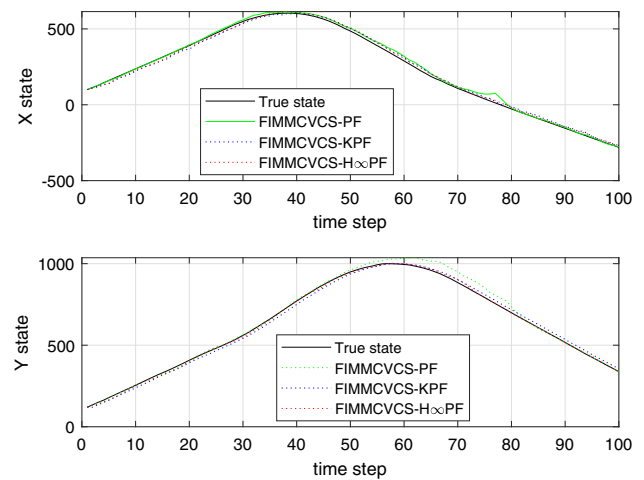
Fig. 13 Trajectory comparison of FIMMCVCS-PF, FIMMCVCS-KPF and FIMMCVCS-$H\infty$PF filter in two axes

than those of FIMMCVCS-KPF and FIMMCVCS-$H\infty$PF. In the entire process of tracking, FIMMCVCS-KPF and FIMMCVCS-$H\infty$PF can all achieve stable tracking, while the tracking error of FIMMCVCS-$H\infty$PF is obviously less than that of FIMMCVCS-KPF, and its tracking performance is still higher than FIMMCVCS-KPF. Because the H-infinity filter generates new particles, and effectively solves the problem of particle starvation, H-infinity filtering algorithm can take into account current measurements and achieve a trade-off between accuracy and robustness.

As is shown in Table 2, we use average magnitude of error and root-mean-square error to evaluate our experimental results, where D-AME is average magnitude of error of distance, X-AME is average magnitude of error in x-axis, Y-AME is average magnitude of error in y-axis, D-RMSE is root-mean-square error of distance, X-RMSE is root-mean-square error in x-axis, and Y-RMSE is root-

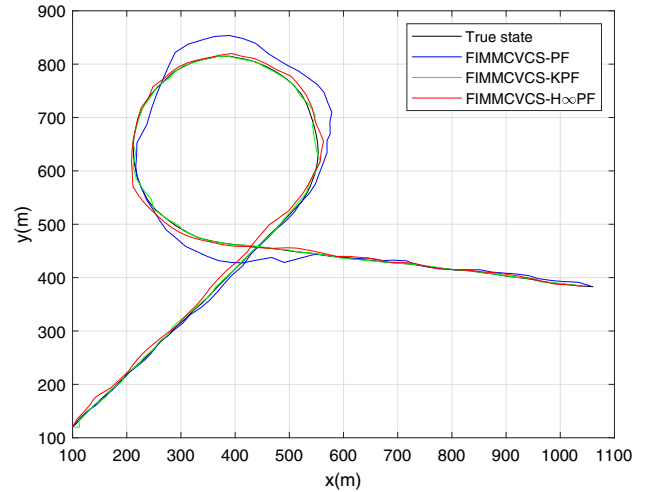**Fig. 14** The position error comparison of FIMMCVCS-PF, FIMMCVCS-KPF and FIMMCVCS-H∞PF.

Fig. 15 Position error comparison of FIMMCVCS-PF, FIMMCVCS-KPF and FIMMCVCS-H∞PF in two axes

mean-square error in y-axis. The AME of FIMMCVCS-H∞PF is reduced nearly half of that of FIMMCVCS-PF and FIMMCVCS-KPF, which indicates that FIMMCVCS-H∞PF has higher precision. The RMSE data shows FIMMCVCS-KPF can keep stable performance, while FIMMCVCS-H∞PF has lower RMSE than FIMMCVCS-KPF and can perform more stable.
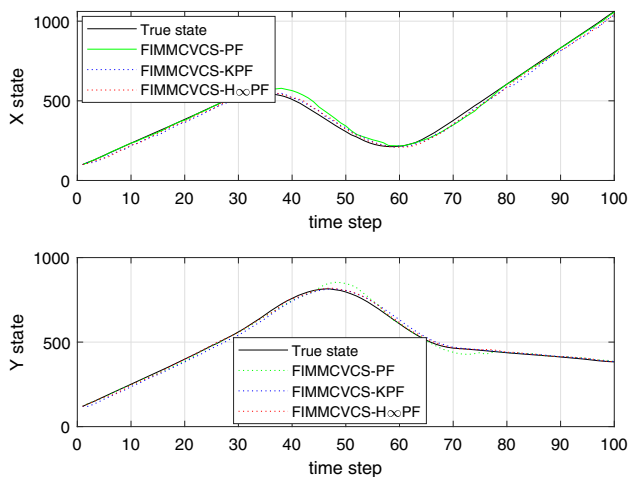

Fig. 16 Trajectory comparison of FIMMCVCS-PF, FIMMCVCS-KPF and FIMMCVCS-H∞PF filter

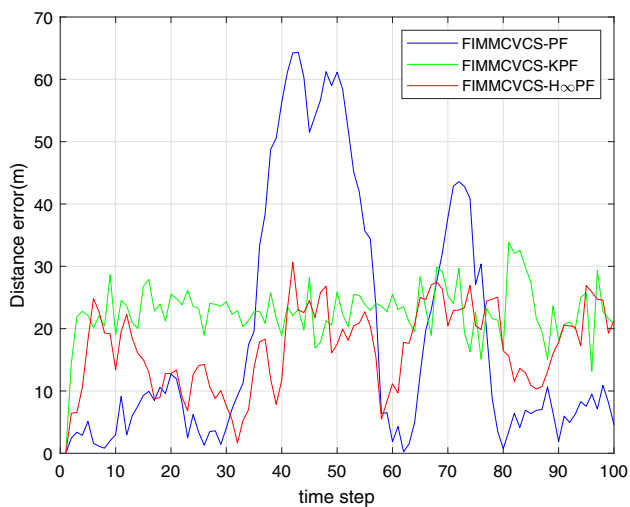### 6.2.2 Strong Maneuvering Target Tracking Situation

In this situation, maneuvering target performs a total of 100 scan cycles, where 1–28 scan cycles are uniform motion, 29–70 scan cycles are turn motion, and the remaining 30 scan cycles are uniform motion. The turn rate is $w = 0.13$ rad/s, and disturbance attenuation factor of $H\infty$ particle filter is $\gamma = 0.7$.

From Figs. 16, 17, 18 and 19, it is seen that FIMMCVCS-$H\infty$PF can still achieve high precision when the target performs lager maneuvering motion. In the entire process of tracking, FIMMCVCS-H∞PF shows the stable tracking performance, and tracking accuracy is better than the other two methods. The tracking performance of FIMMCVCS-KPF is between FIMMCVCS-PF and FIMMcvcs-H∞PF. It is also stable in the whole process. However, its tracking error is relative large to FIMMCVCS-H∞PF, that is, H∞ particle filter can outperform Kalman particle filter. FIMMCVCS-PF can improve tracking performance to some extent when tracking large maneuvering targets, but in the entire process of tracking, when the target happens lager maneuvering, the tracking error of this algorithm is still higher than that of other time. So it cannot achieve stable and accurate tracking for such large maneuvering target.

From Table 3, we can see FIMMCVCS-$H\infty$PF performs better and has lower average magnitude of error and root-mean-square error in x-axis, y-axis and distance than

Table 2 The AME and RMSE of different algorithms in weak maneuvering motion condition	Algorithm	D-AME	X-AME	Y-AME	D-RMSE	X-RMSE	Y-RMSE
	FIMMCVCS-PF	21.6641	11.1430	16.7418	31.9292	16.0258	27.6161
	FIMMCVCS-KPF	22.0228	13.8800	15.7588	22.3404	15.0296	16.5288
	FIMMCVCS-H∞PF	13.5703	11.7806	5.4036	14.5801	12.8047	6.9727

Fig. 17 Trajectory comparison of FIMMCVCS-PF, FIMMCVCS-KPF and FIMMCVCS-H∞PF filter

Fig. 18 The position error comparison of FIMMCVCS-PF, FIMMCVCS-KPF and FIMMCVCS-H∞PF
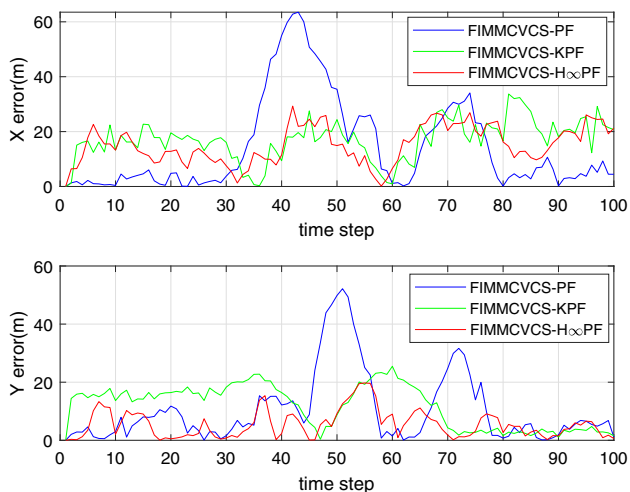
Fig. 19 The position error comparison of FIMMCVCS-PF, FIMMCVCS-KPF and FIMMCVCS-H∞PF in two axes

FIMMCVCS-PF and FIMMCVCS-KPF. It indicates that FIMMCVCS-$H\infty$PF can still achieve high precision and can keep performance stable both in weak maneuvering motion condition and strong maneuvering motion condition.

The track performance improvement comes from these adjustments. We propose an interactive multi-model (FIMM) H-infinity particle filter algorithm based on the "current" statistical model. The model adopted by the proposed algorithm is a "current" statistical model, which can truly reflect the strength of the target maneuver and the range of maneuvering changes. At the same time, the interactive multi-model algorithm can adopt multiple motion models and can accurately reflect the target. The form of motion, and most importantly, the filter in the new algorithm is an H-infinity particle filter. The algorithm achieves accurate and robust tracking throughout the motion of the target.

Model matching probability is one of the factors affecting the tracking performance of IMM algorithm. The model matching probability in the standard IMM algorithm is obtained by the combination calculation method. The method has a large amount of calculation. For this problem, we use a fuzzy control interaction. For this problem, we use a new fuzzy control interaction multi-model based H-infinity particle filtering algorithm. The main improvement of the algorithm is to calculate the model matching probability through fuzzy control theory. The new algorithm reduces the computational complexity of the algorithm to a certain extent and improves the tracking accuracy.

7 Summary

In order to solve the problem of state estimation for nonlinear non-Gaussian systems, this paper proposes a novel fuzzy interacting multiple model $H\infty$ particle filter algorithm based on current statistical model. It can inherit the advantages of the $H\infty$ particle filtering algorithm, and absorb the merits of the IMM algorithm by the fuzzy control theory. So the algorithm can achieve very stable and accurate state estimation performance. The simulation results show that the IMMCVCS-PF algorithm combined with fuzzy control can improve the tracking precision greatly when target performs maneuvering motion. For the IMMCVCS-KPF and IMMCVCS-$H\infty$PF, the fuzzy control theory can also improve the tracking performance to some extent. The three algorithms with the fuzzy control theory can reduce the computational complexity. From the comparisons of the FIMMPF, FIMMCVCS-KPF and FIMMCVCS-$H\infty$PF, we can see that the tracking performance of FIMMCVCS-$H\infty$PF outperforms the other two. Future study will focus on

Table 3 The AME and RMSE of different algorithms in strong maneuvering motion condition

Algorithm	D-AME	X-AME	Y-AME	D-RMSE	X-RMSE	Y-RMSE
FIMMCVCS-PF	19.0395	14.4822	10.4510	27.5556	22.3521	16.1152
FIMMCVCS-KPF	22.6607	16.9804	11.6958	23.0848	18.5156	13.7876
FIMMCVCS-H∞PF	16.8916	15.1203	5.4987	18.1584	16.6303	7.2910

generalizing this method to more difficult scene and we will try to use parallel computing and high-performance computing [23–28] to optimize FIMMCVCS-$H\infty$PF algorithm.

References

1. Radu, V., Yaakov, B., Peter, W.: Multiple-model estimators for tracking sharply maneuvering ground targets. IEEE Trans. Aerospace Electron. Syst. **54**, 1404–1414 (2018)
2. Hadaegh, M., Khaloozadeh, H.: Modified switched IMM estimator based on autoregressive extended Viterbi method for maneuvering target tracking. J. Syst. Eng.Electron. **29**, 1142–1157 (2018)
3. Jiang, Z., Huynh, D.Q.: Multiple pedestrian tracking from monocular videos in an interacting multiple model framework. IEEE Trans. Image Process. **27**, 1361–1375 (2018)
4. Lee, D., Liu, C., Liao, Y., Hedrick, J.K.: Parallel interacting multiple model-based human motion prediction for motion planning of companion robots. IEEE Trans. Autom. Sci. Eng. **14**, 52–61 (2017)
5. Nesrine, A., Nidhal, C., Roman, S.: Souad Chebbi on the convergence of constrained particle filters. IEEE Signal Process. Lett. **24**, 858–862 (2017)
6. Branko, R., Jeremie, H., Sanjeev, A.: Robust target motion analysis using the possibility particle filter. IET Radar Sonar Navig. **13**, 18–22 (2019)
7. Yu, M., Gong, L., Oh, H., Chen, W., Chambers, J.: Multiple model ballistic missile tracking with state-dependent transitions and gaussian particle filtering. IEEE Trans. Aerospace Electron. Syst. **54**, 1066–1081 (2018)
8. Georgia, C., Xanthi, S.P., Costas, S.T., Petros, M.: Augmented human state estimation using interacting multiple model particle filters with probabilistic data association. IEEE Robot. Autom. Lett. **3**, 1872–1879 (2018)
9. Zhang, Y., Wang, S., Li, J.: Improved particle filtering techniques based on generalized interactive genetic algorithm. J. Syst. Eng. Electron. **27**, 242–250 (2016)
10. Xiao, G., Li, K., Zhou, X., Li, K.: Efficient monochromatic and bichromatic probabilistic reverse top-k query processing for uncertain big data. J. Computer Syst. Sci. **89**, 92–113 (2017)
11. Xiao, G., Li, K., Li, K.: Reporting l most influential objects in uncertain databases based on probabilistic reverse top-k queries. Inf. Sci. **405**, 207–226 (2017)
12. Schwiegelshohn, F., Ossovski, E., Hbner, M.: A resampling method for parallel particle filter architectures. Microprocess. Microsyst. **47**, 314–320 (2016)
13. Xiao G., Li K., Chen Y., He W., Zomaya A., Li T.: A customized and accelerative SpMV framework for the Sunway TaihuLight. IEEE Trans. Parallel Distrib. Syst. https://doi.org/10.1109/TPDS.2019.2907537 (2019)
14. Bai A., Simmons R., Veloso, M.: Multi-object tracking and identification via particle filtering over sets. In: Proceedings of the 20th International Conference on Information Fusion, pp. 10–13 (2017)
15. Wang, Q., Li, J., Zhang, M., Yang, C.: H-infinity filter based particle filter for maneuvering target tracking. Prog. Electromagn. Res. B **30**, 103–116 (2011)
16. Shi, P., Zhang, Y., Chadli, M., Agarwal, R.K.: Mixed H-infinity and passive filtering for discrete fuzzy neural networks with stochastic jumps and time delays. IEEE Trans. Neural Netw. Learn. Syst. **27**, 903–909 (2016)
17. Yu, Q., Xiong, R., Lin, C., Shen, W., Deng, J.: Lithium-ion battery parameters and state-of-charge joint estimation based on h-infinity and unscented Kalman filters. IEEE Trans. Veh. Technol. **66**, 8693–8701 (2017)
18. Jia, S., Zhang, Y., Wang, G.: Highly maneuvering target tracking using multi-parameter fusion singer model. J. Syst. Eng. Electron. **28**, 841–850 (2017)
19. Pojala, C., Somnath, S.: Rough-set-theoretic fuzzy cues-based object tracking under improved particle filter framework. IEEE Trans. Fuzzy Syst. **24**, 695–707 (2016)
20. Cosme, L.B., Caminhas, W.M., D'Angelo, M.F., Palhares, R.M.: A novel fault-prognostic approach based on interacting multiple model filters and fuzzy systems. IEEE Trans. Ind. Electron. **66**, 519–528 (2019)
21. Li, L., Xie, W., Liu, Z.: Auxiliary truncated particle filtering with least-square method for bearings-only maneuvering target tracking. IEEE Trans. Aerospace Electron. Syst. **52**, 2562–2567 (2016)
22. Shi, X., Celik, N.: Relative entropy-based density selection in particle filtering for load demand forecast. IEEE Trans. Autom. Sci. Eng. **14**, 946–954 (2017)
23. Xiao, G., Wu, F., Zhou, X., Li, K.: Probabilistic top-k range query processing for uncertain databases. J. Intell. Fuzzy Syst. **31**, 1109–1120 (2016)
24. Li, K., Yang, W., Li, K.: Performance analysis and optimization for SpMV on GPU using probabilistic modeling. IEEE Trans. Parallel Distrib. Syst. **26**, 196–205 (2015)
25. Li, K., Yang, W., Li, K.: Energy-efficient stochastic task scheduling on heterogeneous computing systems. IEEE Trans. Parallel Distrib. Syst. **25**, 2867–2876 (2014)
26. Chen, Y., Xiao, G., Yang, W.: Optimizing partitioned CSR-based SpGEMM on the Sunway TaihuLight. Neural Comput. Appl. (2019). https://doi.org/10.1007/s00521-019-04121-z
27. Chen, Y., Li, K., Yang, W., Xiao, G., Xie, X., Li, T.: Performance-aware model for sparse matrix-matrix multiplication on the Sunway TaihuLight supercomputer. IEEE Trans. Parallel Distrib. Syst. **30**, 923–938 (2019)
28. Li, K., Yang, Z., Xiao, G., Li, K.: Progressive approaches for Pareto optimal groups computation. IEEE Trans. Knowl. Data Eng. **31**, 521–534 (2019)